



# Development of colorimetric cellulose-based test-strip for the rapid detection of antibodies against SARS-CoV2 virus

Bárbara P. Correia · Mariana P. Sousa · Cristina E. A. Sousa · Daniela Mateus · Ana Isabel Sebastião · Maria Teresa Cruz · Ana Miguel Matos · Ana Cláudia Pereira · Felismina T. C. Moreira 

Received: 10 April 2022 / Accepted: 10 August 2022 / Published online: 17 September 2022  
© The Author(s), under exclusive licence to Springer Nature B.V. 2022

**Abstract** Given the pandemic situation, there is an urgent need for an accurate test to monitor antibodies anti-SARS-CoV-2, providing crucial epidemiological and clinical information to monitor the evolution of coronavirus disease in 2019 (COVID-19) and to stratify the immunized and asymptomatic population. Therefore, this paper describes a new cellulose-based test strip for rapid and cost-effective quantitative detection of antibodies to SARS-CoV2 virus by colorimetric transduction. For this purpose, Whatman paper was chemically modified with sodium metaperiodate to introduce aldehyde groups on its surface. Subsequently, the spike protein of the virus is covalently bound by forming an imine group. The

chemical control of cellulose paper modification was evaluated by Fourier transform infrared spectroscopy, thermogravimetry and contact angle analysis. Colorimetric detection of the antibodies was performed by a conventional staining method using Ponceau S solution as the dye. Color analysis was performed after image acquisition with a smartphone using Image J software. The color intensity varied linearly with the logarithm of the anti-S concentration (from 10 ng/mL to 1 µg/mL) in 500-fold diluted serum samples when plotted against the green coordinate extracted from digital images. The test strip was selective in the presence of nucleocapsid antibodies, urea, glucose, and bovine serum albumin with less than 15% interference, and detection of antibodies in human serum was successfully performed. Overall, this is a simple and affordable design that can be readily used for mass

**Supplementary Information** The online version contains supplementary material available at <https://doi.org/10.1007/s10570-022-04808-y>.

B. P. Correia · M. P. Sousa · C. E. A. Sousa · A. C. Pereira · F. T. C. Moreira (✉)  
BioMark/ISEP, School of Engineering, Polytechnic School of Porto, R. Dr. António Bernardino de Almeida, 431, 4249-015 Porto, Portugal  
e-mail: ftm@isep.ipp.pt

B. P. Correia · M. P. Sousa · C. E. A. Sousa · A. C. Pereira · F. T. C. Moreira  
CEB - Centre of Biological Engineering, University of Minho, Braga, Portugal

D. Mateus · A. I. Sebastião · M. T. Cruz · A. M. Matos  
Faculty of Pharmacy, University of Coimbra, 3000-548 Coimbra, Portugal

D. Mateus · A. I. Sebastião · M. T. Cruz  
Center for Innovative Biomedicine and Biotechnology (CIBB), University of Coimbra, 3000-548 Coimbra, Portugal

A. M. Matos  
Chemical Engineering Processes and Forest Products Research Center, CIEPQPF, Faculty of Sciences and Technology, University of Coimbra, 3030-790 Coimbra, Portugal

population screening and does not require sophisticated equipment or qualified personnel.

**Keywords** Colorimetric · Dye · Protein spike · Serum · Test-strips

## Introduction

Over the past 20 years, there have been an increasing number of viral outbreaks, at least five of which have become diseases of global significance: severe acute respiratory syndrome, swine flu (2009), ebola, middle east respiratory syndrome, and the current severe acute respiratory syndrome coronavirus 2 (SARS-CoV-2, 2019) (Roychoudhury et al. 2021). Coronavirus disease 2019 (COVID-19) is caused by the SARS-CoV-2 virus, which emerged in Wuhan, China, in December 2019 and has spread rapidly around the world. Like other coronaviruses, it is composed of several key proteins, including a spike protein (S), a membrane glycoprotein (M), an envelope protein (E), and a nucleocapsid protein (N) that facilitate infection. The spike protein mediates viral entry into host cells by binding to the host angiotensin-converting enzyme 2 (ACE2) receptor and allowing fusion of the viral and host membranes (Li and Liu 2020).

An important step in the treatment and control of a COVID disease is monitoring the human immune response to a SARS-CoV virus. The presence of an immune response and the amount of antibody circulating in the body are often critical tools for assessing a patient's individual condition and disease history, as well as for understanding the mechanisms of regional and global spread of the pathogen (Boechat et al. 2021; Pawliczak 2020).

Serological detection of antibodies has been used as the gold standard for the control and investigation of this pandemic to better monitor population immunity, especially now that vaccination is ongoing in several countries. These tests are considered user-friendly but have limited sensitivity and require at least two antibodies for detection (Galipeau et al. 2020; Guevara-Hoyer et al. 2021; Jacot et al. 2021; Paradiso et al. 2020). In addition, the most commonly used serologic laboratory tests are based on enzyme-linked immunosorbent assays (ELISA), automated chemiluminescence tests (Klupfel et al. 2021; Paul et al. 2021), neutralization tests (Embregts et al.

2021; Rathe et al. 2021) and rapid immunoassays (Findeisen et al. 2021). With the exception of rapid tests, all test systems require a large amount of time and qualified personnel to perform the analysis and interpret the results, making these tests inappropriate when a large number of tests are needed immediately. These limitations highlight the urgent need to develop simple and affordable rapid tests for the point-of-care (PoC) setting (Di Domenico et al. 2021; Huang et al. 2004; Jacot et al. 2021; Lee et al. 2008).

Biosensors are considered a promising alternative to serological tests because they allow PoC analysis, usually offer a rapid response, can be miniaturized, and are generally inexpensive. However, these devices require a power supply and additional equipment for readout. Several electrochemical biosensors have been described in the literature for the detection of antibodies to SARS-CoV2 in PoC (Fani et al. 2021; Imran et al. 2021; Szunerits et al. 2022).

Cellulose paper has been used as a substrate for sensory applications since the nineteenth century. Urine and pH test strips have been widely used in this context. This material has proven to be very important as a support material for the separation of components of a complex matrix, for example in techniques such as chromatography and electrophoresis, and has become a rapidly growing market material (Imamura et al. 2020). Cellulose is an excellent resource because its renewability, recyclability, and biodegradability fitting the concept of green chemistry, and it is also one of the most widely produced biopolymers on Earth. The most common method using cellulose as a support material is the lateral flow test (LFT) (Peto and Uk 2021; Sibai et al. 2021; Wang et al. 2021). These tests have a faster reaction time compared to ELISA, but they are also expensive because two antibodies are needed, one of which is modified with a nanoparticle or enzyme. In addition, LFT tests do not provide a quantitative antibody response, only qualitative information.

A promising alternative to LFT are the well-known dipsticks, which resemble urine test strips. In practice, dipstick analysis involves dropping a sample onto different sections of a dipstick, which causes a timed reaction, and then comparing the color change of the dipstick to a reference standard to determine a positive or negative result. The color change is usually triggered by the reaction of a chromogenic compound with another reaction product resulting from

the interaction between the sample and the dipstick reagent. Other common chemical reactions include dye binding, enzymatic, immunological, and catalytic oxidation–reduction reactions (Kavuru et al. 2020). Overall, the main advantage of using test strips is quantitative analysis, where the intensity of the color change is proportional to the concentration of the analyte measured. The color is then compared to a color reference chart to subjectively measure the concentration of the analyte. These manual/visual evaluations can be inaccurate. To overcome this limitation, software could be used to capture and analyze the images.

Overall, this paper reports, for the first time, the development of a test strip on a cellulose support for rapid and quantitative detection of antibodies to SARS-CoV2 by visual comparison of color change. For this purpose, the cellulose paper is chemically modified by metaperiodate treatment to introduce aldehyde groups for further covalent binding of bio-recognition elements. Color detection was performed with a conventional staining solution using Ponceau S solution. The color changes were recorded with a smartphone RGB camera and then the intensity increase was determined. As a result, a quantitative relationship was successfully established between the antibody concentrations and the color intensity values of the captured images. The high accuracy of this method was demonstrated when measuring real serum samples with a linear response ranging from 10 ng/mL to 1 µg/mL. This technology has great potential as a PoC platform for screening COVID or immunity of vaccinated individuals. Importantly, this concept can be easily adapted to another pathology that may arise in humankind.

## Experimental section

### Materials and methods

#### *Apparatus*

Fourier transform infrared spectroscopy (FTIR) measurements were performed using a Nicolet 6700 FTIR spectrometer. The infrared spectra were recorded at room temperature after background correction. The number of scans was 80 for both sample and background. The X-axis corresponds to the wavelength, which is between 500 and 4000  $\text{cm}^{-1}$ , and the

Y-axis corresponds to the percent transmittance. The thermal behavior of the different modification steps of the test strips was evaluated using the thermogravimeter (TG)/differential thermal analyzer (DTA) Exstar TG/DTA 7200. The contact angle of the different modification steps was measured by dropping 20 µL of water onto the paper surface and reading the respective angle with the Image J program.

For color analysis, the program Image J was used, which evaluates the RGB coordinates of the color system (red, green and blue).

The photos were taken with a smartphone with a 12-megapixel camera and an aperture lens of f/2.4. All photos were taken in the same room and in the same place to ensure the same characteristics and conditions regarding temperature and sunlight exposure. Additionally, a white sheet under all tested strips was used to ensure the same background.

#### *Reagents*

All reagents were of analytical grade and aqueous solutions were diluted with ultrapure water (conductivity < 0.1 µS/cm). Whatman paper N°40 (thickness 210 nm), sodium metaperiodate ( $\text{NaIO}_4$ ) was purchased from VWR. CORMAY serum, recombinant SARS-CoV-2 spike (S) glycoprotein and the corresponding antibody were purchased from Sigma-Aldrich, phosphate salt buffer (PBS) from VWR, and MES monohydrate 98% from AppliChem. Ponceau S solution was obtained from Sigma-Aldrich and glacial acetic acid from Carlo Erba. Glucose was from Alfa Aesar, urea from Fagron, bovine serum albumin (BSA) from Sigma-Aldrich, and human antibody to SARS-CoV-2 nucleocapsid (5000 ng/mL) from Abcam.

#### Chemical modification of the cellulose

The cellulose papers were cut into circles of 0.6 cm in diameter and washed with 25 mL of absolute ethanol for 30 min with moderate stirring to remove some organic compounds on the surface. For chemical modification (Fig. 1), the washed Whatman paper was then oxidized with sodium metaperiodate at different concentrations (mol/L): 0.05, 0.1, 0.4 and 0.5 for 1, 2, 3, 4 and 24 h, respectively. The incubation temperature ( $^{\circ}\text{C}$ ) 110, 90, 60, 37 and the influence of

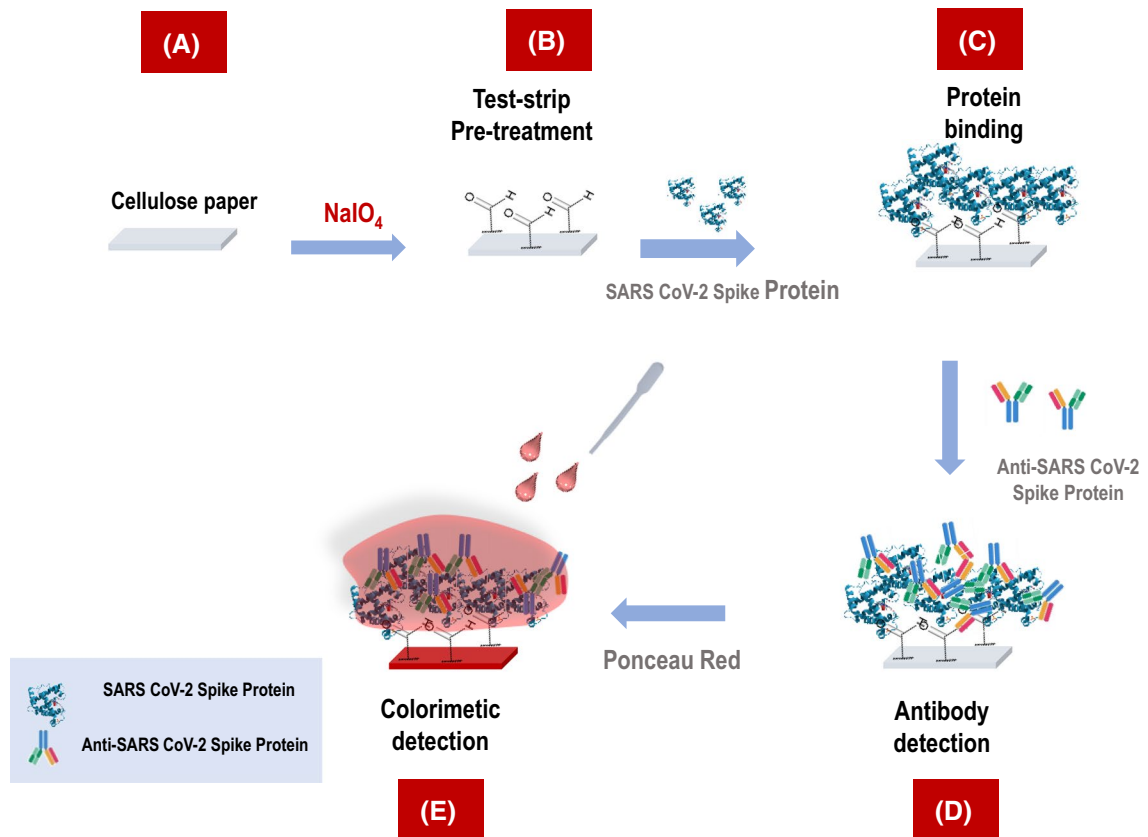


**Fig. 1** Scheme representing a synthesis of a colorimetric sensor on cellulose paper, where: **A** represents the paper followed by pre-preparation with absolute ethanol and chemical modification with the formation of an aldehyde group on cellulose

paper (**B**); **C** represents the immobilization of spike protein antigen of virus, **D** immobilization of respective antibody and **E** represents the color revelation with solution Ponceau S solution

the presence and absence of stirring during the oxidation process were also evaluated.

Overall, the best experimental conditions for the functionalization of cellulose paper were achieved during overnight incubation with 20  $\mu\text{L}$ , 0.5 mol/L  $\text{NaIO}_4$  (solution prepared the same day) at room temperature and protected from light. To remove excess metaperiodate, the papers were washed in deionized water for 10 min, then pre-dried on absorbent paper and incubated at 37  $^\circ\text{C}$  for three hours. The success of the chemical modification of the paper was evaluated by infrared absorption spectra (FTIR).

To study the binding of the recognition element (Fig. 1), a solution of the spike protein (S) (5  $\mu\text{g}/\text{mL}$ ) was prepared in PBS at different pH values (5, 7 and 10), since pH is a parameter that significantly affects protein conformation and protonation. The solutions were incubated overnight with the chemically

modified papers. Subsequently, the protein that had not covalently bound to the sensor surface was washed with 30  $\mu\text{L}$  of PBS at pH 5 and allowed to dry at room temperature.

#### Detection and quantification of the anti-SARS-CoV2 antibodies

The resulting sensor S/ $\text{NaIO}_4$ /cellulose was then incubated with increasing concentrations of human anti-SARS-CoV2 polyclonal antibody between 100 ng/mL and 50  $\mu\text{g}/\text{mL}$  at pH 5 for 30 min at room temperature. After incubation, the papers were washed with buffer at pH 5, and the detection and quantification of target antibodies associated with the biosensor were examined by the classical method of staining with Ponceau S solution (0.1% (v/v) in 5% acetic acid). In this method, cellulose was immersed in 5 mL of the

staining solution for 2 s to promote color development and then immediately immersed in a distillation solution of 10% (v/v) acetic acid in deionized water to remove excess dye. Color development was observed for 15 min and then dried with absorbent paper to remove excess solvent. Colors were captured using the camera of a smartphone, which allowed evaluation of the biosensor performance by recording and quantifying the color coordinates of each captured image using the RGB (red, green, and blue) color system of the Image J program. After optimization, the Cormay serum samples were tested with different dilution factors, one thousand-fold and five 100- fold.

### Selectivity study

The selectivity study was performed by incubating different compounds present in synthetic human serum to evaluate the percentage (%) of interference by RGB coordinates. The interfering substances selected were diluted in buffer at (pH 5) and were BSA (1 mg/mL), glucose (0.7 mg/mL), urea (0.2 mg/mL), and human SARS-CoV-2 nucleocapsid glycoprotein antibody (5000 ng/mL). For each modified paper incubated with the different interference agents selected, the relative error was determined using the RGB coordinates with the Image J program. Percent interference was calculated using the following formula: (% interference =  $[\text{anti-S} - (\text{anti-S} + \text{interference agent})/\text{anti-S}]$ ). All the assays were performed in triplicate.

### Reproducibility study

Sensor reproducibility is a relevant parameter in sensor evaluation. In this way, the sensor performance was evaluated over different construction days. This performance was evaluated by incubating different concentrations of prepared target in buffer and analysing the respective RSD value. All the assays were performed in triplicate.

### Analysis of spiked serum samples

Anti-S standard solutions were prepared by 500-fold dilution of synthetic serum in buffer MES (pH 5). The relative error was classified by analyzing an

image from the three replicates and evaluating the RGB coordinates of the Image J program using the green coordinate. All the assays were performed in triplicate.

### Analysis of real samples

The samples from patients tested positive for SARS-CoV2 were collected under the routine blood analysis performed by the Clinic Pathology Service from the University Hospital of Coimbra. This study was previously approved by the Ethics Commission to Clinical Investigation, under the reference OBS. SF.220-2021.

Immunoassay tests were executed by VIDAS® SARS-CoV2 IgG from Biomérieux (Marcy l’Etoile, France) to quantify IgG antibodies against SARS-CoV2 S protein in human serum samples, allowing to select samples with different concentrations of antibodies to be further tested in the new cellulose-based test strip. VIDAS® SARS-CoV2 IgG performs an automated qualitative enzyme-linked immunosorbent assay (ELISA) to detect specific IgG anti-SARS-CoV2 that are present in the collected human serum and the VIDAS SARS-CoV2 IgG 423,834-02® kit (BioMérieux, Marcy l’Etoile, France) was used. This kit includes the single-use solid-phase strips, solid-phase receptacles that contain humanized recombinant anti-SARS-CoV-2 antigen, the standard (including a humanized recombinant anti-SARS-CoV-2 IgG antibody), and the positive (containing, also, a humanized recombinant anti-SARS-CoV-2 IgG antibody) and negative controls (which does not include the humanized recombinant anti-SARS-CoV-2 IgG antibody) (<https://www.biomerieux-diagnostics.com/vidas-sars-cov-2>). To quantify the human samples, solutions obtained from sequential dilutions of the purified anti-SARS-CoV-2 S protein S1 recombinant antibody (BioLegend, San Diego, CA, USA) were used to establish a standard curve.

The positive human serum samples were incubated, in triplicate, with various modified cellulose papers. Serum was prepared by five-100-fold dilution in buffer (pH 5). By analyzing the RGB coordinates, the intensity of the color on the paper was determined with positive and negative samples to validate the colorimetric sensor.

## Results and discussion

### Surface modification

Cellulose membranes were chemically modified according to the scheme shown in Fig. 1. The first step consisted of (1) formation of an aldehyde layer, followed by (2) protein binding. In the chemical modification, the cellulose surface was first oxidized with sodium metaperiodate to generate aldehyde groups ( $-\text{CHO}$ ) on the sensor surface. The action of this compound on the cellulose resulted in the opening of the D-glucose rings by converting the hydroxyl groups of C2 and C3 to carbonyl groups (Kristiansen et al. 2010). In the chemical modification of cellulose paper, it was found that the distribution of the aldehyde group changed the physicochemical properties of the paper. The reduction of crystallinity and shrinkage of the paper were the main differences that contributed to the evidence of chemical modification of cellulose paper. During the optimization processes, it was also found that as the oxidation time increased, the contact of the strips with the sodium metaperiodate increased and consequently the geometric area of the paper decreased. The thickness also increased slightly. Overall, it is important to note that these changes in the chemical structure of the paper are visible to the naked eye and can be verified by characterization methods.

A 24-h oxidation, protected from light and at room temperature, were therefore the optimal conditions for the next step. The functionalized surface was then incubated after 24 h with protein S at a concentration of  $5 \mu\text{g/mL}$  at (pH 5). This last step allowed the covalent bonding of the aldehyde groups on the oxidized paper with the amine groups of the protein, forming a Schiff surface (imine binding). Finally, the sensor was washed with buffer solution (pH 5, PBS) to remove unbound protein.

### Characterization of the surface modification

#### FTIR

Paper oxidation by metaperiodate was analyzed, optimized, and characterized using Fourier transform infrared spectroscopy (FTIR). Figure 2 shows the FTIR spectroscopy analysis performed for the cellulose paper, with the changes detected in the chemical modification of the paper shown in blue and red. When analyzing the spectra, one can observe the appearance of a stretching band ( $\text{C}=\text{O}$ ) in the region of  $1730 \text{ cm}^{-1}$  in the red spectrum. This band is characteristic of an aldehyde formed by carbonyl bonds along the cellulose fibers. Compared to the blue spectrum of the cellulose paper, an increase in the intensity of the vibrational peak was observed at  $1637 \text{ cm}^{-1}$  is attributed to the carbonyl groups from the chemical oxidation of the glucose. In general, the

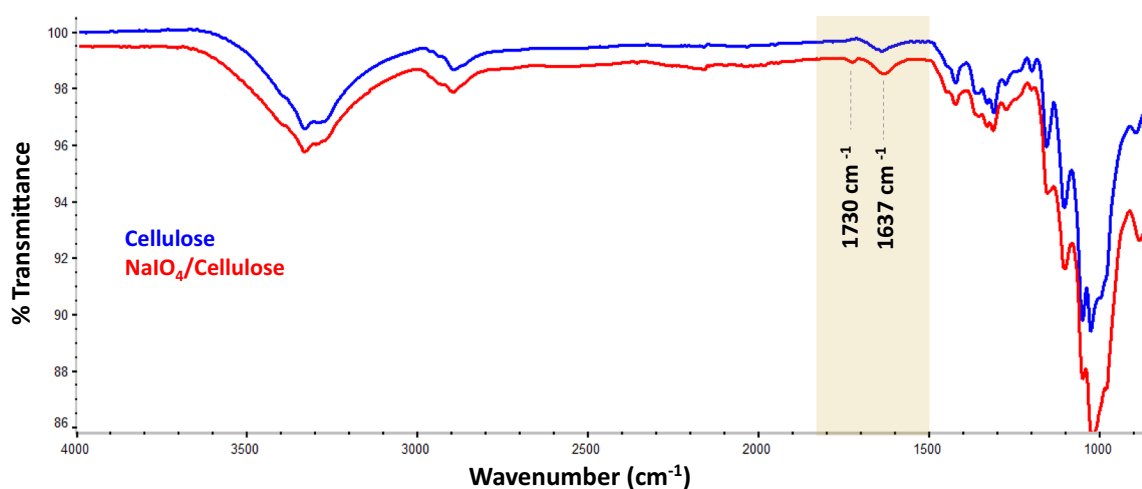


**Fig. 2** FTIR spectra of different immobilization steps of the sensor. The (blue) curve represents the spectra the Cellulose paper and the (red) refers to Cellulose functionalized with metaperiodate of sodium ( $\text{NaIO}_4$ )



interpretation of the FTIR bands shows that there are chemical differences between the cellulose paper and the  $\text{NaIO}_4$ /cellulose sensor.

### Contact angle

Contact angle is a strategy for characterizing the paper surface at each step of biosensor construction. In general, this technique evaluates the intensity with which liquid molecules interact on a solid surface. Figure S1 shows the contact angle for the following steps of this process: (A) cellulose paper, (B)  $\text{NaIO}_4$ /cellulose, and (C) protein S/ $\text{NaIO}_4$ /cellulose.

This process measures the angle formed by a drop of deionized water on the surface of the cellulose paper within 20 s. In the literature, a contact angle between  $90^\circ$  and  $150^\circ$  on the solid surface under study is called hydrophobic, while angles above  $150^\circ$  are called superhydrophobic (Yin et al. 2018). Thus, surface analysis of the paper pre-treated with absolute ethanol yielded a contact angle of ( $\theta = 54.89^\circ \pm 3.26$ ), a value corresponding to the lowest of the three levels listed in the figure. This is due to the porous structure of the cellulose, which allows a high level of absorption of the added water droplet (A). In the next step, the surface functionalized with sodium metaperiodate (B) limited the hydrophobic properties by repelling the treated water droplet, and the highest contact angle was recorded with a value of ( $\theta = 77.98^\circ \pm 3.49$ ). The hydrophilicity of cellulose can be modified by the addition of substances that add other properties and facilitate the introduction of specific chemical groups that improve the compatibility between charge and matrix. Treatment with sodium metaperiodate allows chemical functionalization due to the presence of hydroxyl groups of the  $\beta$ -D-glucopyranoside, which are converted into carbonyl groups, leading to disruption of the cellulose structure, resulting in a decrease in crystallinity (Yin et al. 2018). In addition, long oxidation periods reduce the capillarity of liquids by reducing the hydrogen bonds between the water molecules and the hydroxyl groups, making it more difficult for water to be absorbed onto the exposed paper (Imamura et al. 2020). Overall, the oxidation of the cellulose paper provided with this methodology decreases hydrophilicity due to the loss of hydroxyl groups, resulting in a higher contact angle.

After the chemical modification step, the addition of the S-protein on the paper surface decreases the hydrophobic character, leading to a decrease in the contact angle. In addition, the hydrophilic residues of the protein have an affinity for water molecules, and their interaction leads to a lower contact angle (C) of ( $\theta = 65.32^\circ \pm 2.91$ ). All the assays were performed in triplicate.

### TG analysis

Thermogravimetric methods allow the determination of thermal stability properties of chemically modified cellulose paper at different stages of biosensor construction. Among the different analytical methods, the thermograms of mass loss (TG) and its first derivatives (DTG) at  $550^\circ\text{C}$  were evaluated.

Figure S2 shows the thermograms of the different fabrication steps, where the light blue curve shows the cellulose paper, the red curve shows the paper chemically modified with sodium metaperiodate, and the dark blue curve shows the test strip after covalent binding of protein S. Thermal decomposition occurred at approximately the same temperatures for all modification steps with a maximum shift of  $38^\circ\text{C}$ . The most severe decomposition was observed in cellulose paper, which started at  $314.74^\circ\text{C}$  and ended at  $371.77^\circ\text{C}$ , with a weight loss of 81.98%. When the cellulose paper was modified with  $\text{NaIO}_4$ , a mass loss of 43.18% was observed. When the test strips previously modified with  $\text{NaIO}_4$  then reacted with protein S, a total mass loss of approximately 30.90% was observed (DTG and TG graphs).

Moreover, analysis of TG allows confirmation of cellulose modification once it is possible to observe different degradation rates at each modification step. From the light blue curve (unmodified cellulose paper), it can be concluded that the main degradation occurred between 200 and  $360^\circ\text{C}$ . After periodate treatment (red curve), thermostability decreased in the lower temperature range (0 and  $360^\circ\text{C}$ ), while it increased in the upper temperature range (360 and  $550^\circ\text{C}$ ). Overall, the degradation of oxidized cellulose was observed at two different temperatures (200 and  $300^\circ\text{C}$ , respectively). Moreover, a lower weight loss was observed at  $360^\circ\text{C}$  than for non-oxidized cellulose. This behavior was attributed to the lower crystallinity of the oxidized samples and to degradation reactions during periodate oxidation. After

protein attachment (dark blue curve), thermostability decreased compared to periodate modification due to the presence of covalently bound protein. Degradation was observed at three different temperatures (at 200, 220, and 300 °C, respectively). The additional degradation at 220 °C is related to the presence of organic compounds due to the presence of the protein. Overall, thermogravimetric analysis showed the presence of available aldehyde on the sensor surface after its functionalization. All the assays were performed in triplicate.

#### Detection and quantification of the Anti-S

Detection and quantification of target antibodies bound to the protein S/NaIO<sub>4</sub>/cellulose sensor was determined by a conventional staining method. The colorimetric response of the anti-spike antibody biosensor (anti-S) was monitored after incubation for 30 min at room temperature with 15 μL of different polyclonal anti-body-S standard solutions prepared in buffer at pH=5. Subsequently, the biosensor was washed with 60 μL of PBS (pH 5), and as a reaction

of the test strip, the papers were briefly dipped in the staining solution Ponceau S Solution after washing, which is commonly used for the detection and quantification of proteins.

The final step was immediate immersion in a distillation solution to remove the excess unreacted dye in the sensor. Ponceau S binds specifically to the protein present through an electrostatic interaction, resulting in a red stained area on the paper where the protein is bound. Since this staining solution reacts with protonated amines, pH=5 was used in all phases instead of pH=7, since the isoelectric point of protein S is approximately 7. Color analysis was recorded using a smartphone camera, and naked eye color comparison and RGB coordinate analysis were performed for each standard using Image J software (Fig. 3). All the assays were performed in triplicate and the average of the relative standard deviation (RSD) of the coordinate green was 5%.

With the naked eye, it could be observed in Fig. 3 that there is a variation in the green coordinate and that the intensity of the reddish color increases proportionally with the increase in the amount of target

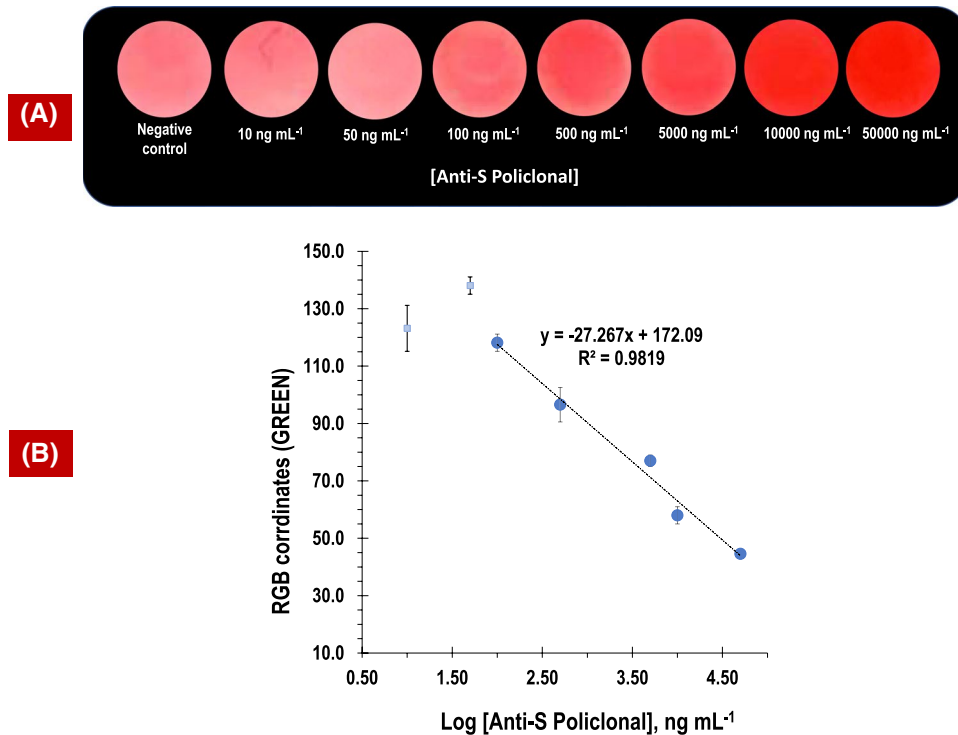


**Fig. 3** Calibration was defined for standard solutions with different concentrations from 10 ng mL<sup>-1</sup> to 50 μg mL<sup>-1</sup>



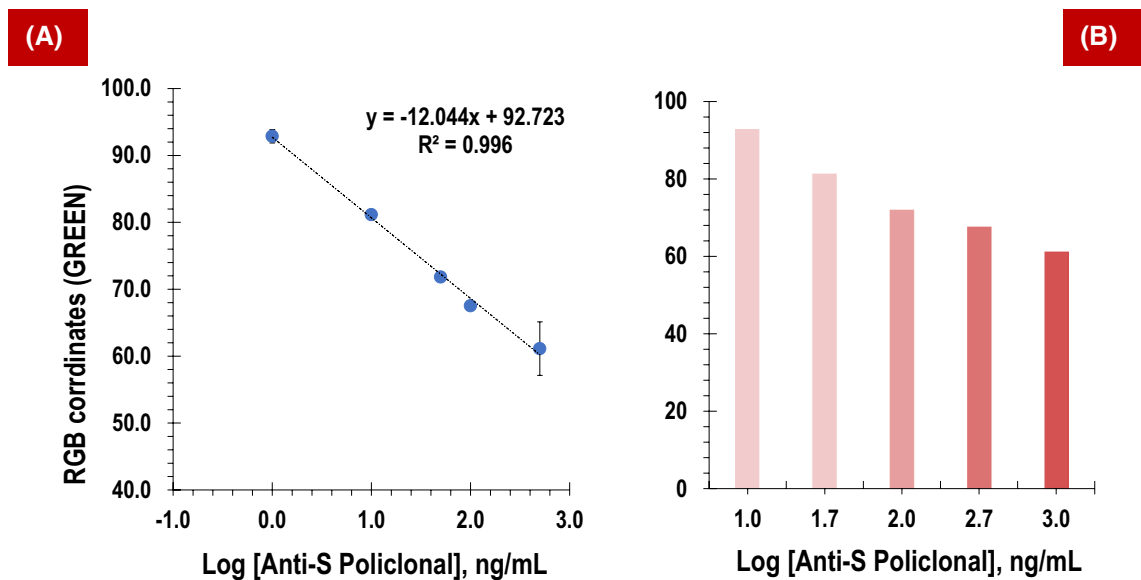


**Fig. 4** Calibration curve of the polyclonal antibody spike protein in  $500 \times$  diluted Cormay serum (pH 5). The concentrations of the spike protein polyclonal antibodies used ranged from 10 to 1000 ng/mL

antibody on the sensory surface. The LOD was calculated similar to direct potentiometric measurements based on the Nernst equation, which is a semi-logarithmic relationship between the electrochemical potential and the logarithm of the concentration. The LOD was 31.6 ng/mL and corresponds to the concentration of the cross section of the two linear parts of the reaction. Overall, the biosensor shows a linear behavior within 100 ng/mL to  $50 \times 10^{-6}$  mL $^{-1}$  with a correlation coefficient of 0.9943.

Next, using the same method, calibration was performed with the synthetic human Cormay serum with increasing antibody concentrations (Fig. 4A). For this purpose, the serum was first diluted 500-fold in MES buffer at pH 5, and standard solutions of polyclonal anti-S were prepared in the diluted serum, ranging from 10 ng/mL to 1.0  $\mu$ g/mL. Again, Image J software was used to analyze color development as a function of the different concentrations. Overall, the biosensor showed a linear response ranging from 10 ng/mL to 1.0  $\mu$ g/mL, with a correlation coefficient of 0.9876. All assays were performed in triplicate and the average of the RSD of the coordinate green was 1.6%.

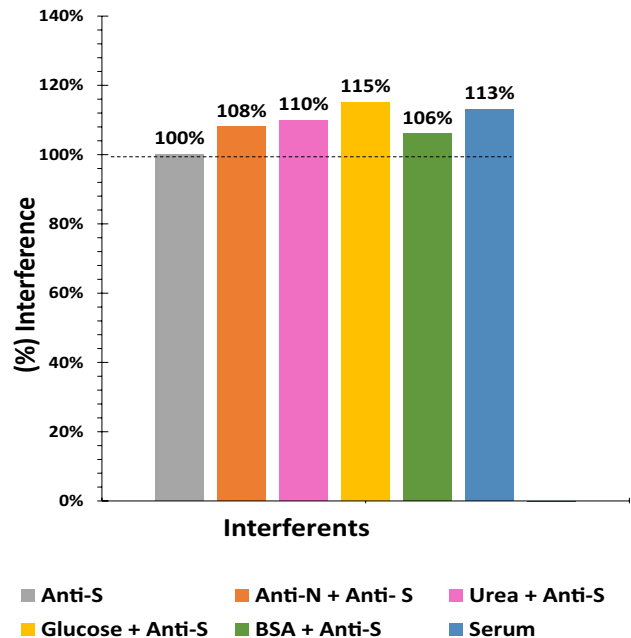
Overall, compared to several biosensors described in the literature, especially optical and electrochemical ones, this colorimetric device based on a paper

test strip offers the great advantage of independence from conventional measuring devices, as it allows the detection of color differences with the naked eye, which is advantageous from an economic point of view. Moreover, this biosensor sustainably allows the immobilization of proteins as a recognition element and the detection of different and very low amounts of antibodies with detection limits in the range of ng/mL. This biosensor could achieve good analytical performance in terms of selectivity, sensitivity, stability, speed, quantification and colorimetric signal detection.

#### Selectivity study

Selectivity tests were then performed to evaluate the ability of the sensor to distinguish antibody S from other species present in biological fluids. In this way, fixed concentrations of the antibody on the sensor surface was incubated together with different interfering species at concentrations corresponding to normal physiological conditions. This study was performed with antibody S (5000 ng/mL), glucose (0.7 mg/mL), urea (0.2 mg/mL), BSA diluted five 100-fold in PBS buffer, pH 5 (1 mg/mL), and nucleocapsid antibody (anti-N) (5000 ng/mL) (Fig. 5). Incubation was performed at room temperature for 30 min, and the

**Fig. 5** Selectivity study involving the analysis of the response of the sensor after 30 min incubation with buffer and other interfering species. The interferers were: (BSA (1 mg/mL) Glucose (0.7 mg/mL), urea (0.2 mg/mL) and humanized antibodies of SARS-CoV-2 nucleocapsid glycoprotein (5000 ng/mL) and human serum 500-fold diluted)



respective interfering substances were prepared in buffer containing pH 5. It was found that each interfering substance slightly affected the colorimetric signal. The average deviation (%) of the color produced by each interfering substance compared to the control (anti-S) was  $15\% \pm 1\%$ , for glucose,  $10\% \pm 2\%$ , for urea,  $6\% \pm 2\%$ , for BSA and 8% for anti-N and human serum 500 diluted ( $113 \pm 2\%$ ),

Thus, the sensor proved to be specific for the determination of anti-S in synthetic human serum. All the assays were performed in triplicate.

#### Validation of the paper test strip

##### *Analysis of spiked serum samples*

The standard addition method was applied to determine Anti-S in synthetic human serum samples spiked with 10 ng/mL of antibody-S. The assay was performed in triplicate and analyzed by RGB coordinates from the *program Image J*. The RSD obtained for reproduced assays was 13%.

##### *Analysis of real samples*

As aforementioned, VIDAS® is a qualitative instrument (<https://www.biomerieux-diagnostics.com/vidas-sars-cov-2>). In order to quantify human

samples relatively to their concentration of anti-S SARS-CoV-2 IgG, a standard curve relating the logarithm of the concentration of the antibody ( $\mu\text{g/mL}$ ) with the relative fluorescence value (RFV—Fig. S4) was established using different concentrations of purified anti-SARS-CoV-2 S1 protein recombinant antibody. The anti-S SARS-CoV-2 IgG concentration present in the real samples was calculated by intersecting the obtained RFV on the curve. This allowed a perception of the range of anti-S protein IgG antibody concentrations on the samples present amidst the COVID-19 positive population, to be further used in our cellulose-based test strip.

Then, the validation of the colorimetric sensor on paper strips was tested with the positive real human serum. For this purpose, a fixed concentration of  $176 \mu\text{g} / \text{mL}$ , diluted in a five 100- fold, was incubated in the sensor for 30 min (Fig. 6). The corresponding negative real human serum was prepared in five 100- fold dilutions in buffer at pH 5. The assay was performed in triplicate and analyzed using the RGB coordinates of the *Image J* program (Fig. S4). Analysis using the green coordinate allowed the difference in hue visible to the naked eye between true positive and negative samples clearly seen, as shown in the Fig. S4. The determined error was precisely 4%. The paper strip sensor is thus able to determine and validate true

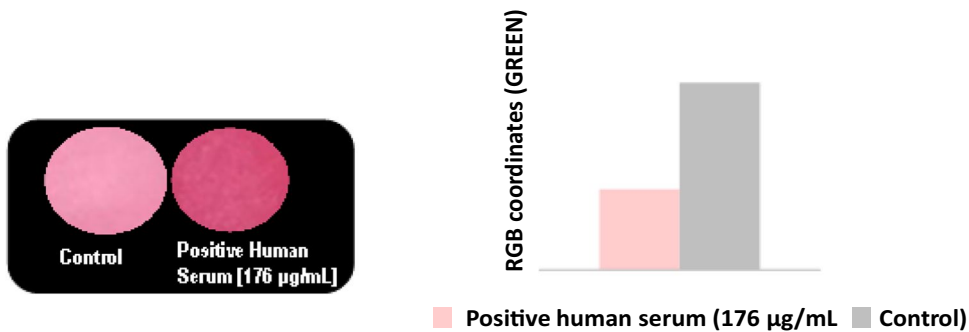


**Fig. 6** Paper-based sensor evaluation with positive human serum diluted five hundred times in PBS (pH = 5) after 30 min incubation at a concentration of 176 µg/mL

samples and distinguish whether the patient serum sample is positive or negative.

## Conclusion

In this work, a colorimetric paper sensor for the detection of antibodies against the spike protein of SARS-CoV-2 was presented. The chemical modifications provided the necessary aldehyde functional groups to immobilize the SARS-CoV-2 spike glycoprotein, which served as a recognition element. The performance of the sensor allowed the concentration of the target to be correlated with a colorimetric response of the recognition agent, both in buffer and in synthetic serum. The sensor showed a linear range with the naked eye; indeed, Fig. 3A shows that there is a variation in the green coordinate and that the intensity of the reddish color increases proportionally with the increase in the amount of target antibody on the sensory surface. Overall, the biosensor shows a linear behavior within  $100 \text{ ng mL}^{-1}$ – $50 \text{ µg mL}^{-1}$  in PBS buffer and  $100 \text{ ng mL}^{-1}$  to  $50 \text{ µg mL}^{-1}$  in spiked serum samples with a correlation coefficient of 0.994, Fig. 3B.

In addition, the device provided good selectivity when tested with solutions containing both the target and interfering molecules. The percentage of interference recorded in relation to the control (anti-S) was 15% for glucose, 10% for urea, 6% for BSA and 8% for anti-N. The preliminary results with real samples showed that the sensor responds well in complex matrices and therefore has the potential to be used in a clinical context.

With this technology will be possible to evaluate the immune response to natural infection as well

as vaccination in a population. Overall, the sensor design meets PoC requirements and represents an affordable, portable, device-free instrument for population screening at a time when mass testing is essential for disease outbreak control.

**Funding** This project was a financially supported through the project, TecniCov (POCI-01-02B7-FEDER-069745), co-funded by FEDER through COMPETE2020 and Lisboa2020.

## Declarations

**Conflict of interest** The authors have not disclosed any competing interests.

## References

- Boechat JL, Chora I, Morais A, Delgado L (2021) The immune response to SARS-CoV-2 and COVID-19 immunopathology: current perspectives. *Pulmonology* 27(5):423–437. <https://doi.org/10.1016/j.pulmoe.2021.03.008>
- Di Domenico M, De Rosa A, Boccellino M (2021) Detection of SARS-COV-2 proteins using an ELISA test. *Diagnostics* 11(4):698. <https://doi.org/10.3390/diagnostics11040698>
- Embregts CWE, Verstrepen B, Langermans JAM, Boszormenyi KP, Sikkema RS, de Vries RD, Hoffmann D, Wernike K, Smit LAM, Zhao S, Rockx B, Koopmans MPG, Haagmans BL, Kuiken T, GeurtsvanKessel CH (2021) Evaluation of a multi-species SARS-CoV-2 surrogate virus neutralization test. *One Health* 13:100313. <https://doi.org/10.1016/j.onehlt.2021.100313>
- Fani M, Zandi M, Soltani S, Abbasi S (2021) Future developments in biosensors for field-ready SARS-CoV-2 virus diagnostics. *Biotechnol Appl Biochem* 68(4):695–699. <https://doi.org/10.1002/bab.2033>
- Findeisen P, Stiegler H, Lopez-Calle E, Schneider T, Urlaub E, Hayer J, Zemmrich C (2021) Clinical performance

- evaluation of a SARS-CoV-2 rapid antibody test for determining past exposure to SARS-CoV-2. *Int J Infect Dis* 103:636–641. <https://doi.org/10.1016/j.ijid.2020.11.164>
- Galipeau Y, Greig M, Liu G, Driedger M, Langlois MA (2020) Humoral responses and serological assays in SARS-CoV-2 infections. *Front Immunol* 11:1–19. <https://doi.org/10.3389/fimmu.2020.610688>
- Guevara-Hoyer K, Fuentes-Antras J, De la Fuente-Munoz E, de la Pena AR, Vinuela M, Cabello-Clotet N, Estrada V, Culebras E, Delgado-Iribarren A, Martinez-Novillo M, Torreon MJ, de Diego RP, Fernandez-Arquero M, Ocana A, Perez-Segura P, Sanchez-Ramon S (2021) Serological tests in the detection of SARS-CoV-2 antibodies. *Diagnostics* 11(4):1–10. <https://doi.org/10.3390/diagnostics11040678>
- Huang LR, Chiu CM, Yeh SH, Huang WH, Hsueh PR, Yang WZ, Yang JY, Su IJ, Chang SC, Chen PJ (2004) Evaluation of antibody responses against SARS coronavirus nucleocapsid or spike proteins by immunoblotting or ELISA. *J Med Virol* 73(3):338–346. <https://doi.org/10.1002/jmv.20096>
- Imamura AH, Segato TP, de Oliveira LJM, Hassan A, Crespielho FN, Carrilho E (2020) Monitoring cellulose oxidation for protein immobilization in paper-based low-cost biosensors. *Mikrochim Acta* 187(5):272. <https://doi.org/10.1007/s00604-020-04250-6>
- Imran S, Ahmadi S, Kerman K (2021) Electrochemical biosensors for the detection of SARS-CoV-2 and other viruses. *Micromachines* 12(2):1–23. <https://doi.org/10.3390/mi12020174>
- Jacot D, Moraz M, Coste AT, Aubry C, Sacks JA, Greub G, Croxatto A (2021) Evaluation of sixteen ELISA SARS-CoV-2 serological tests. *J Clin Virol* 142:104931. <https://doi.org/10.1016/j.jcv.2021.104931>
- Kavuru V, Vu T, Karageorge L, Choudhury D, Senger R, Robertson J (2020) Dipstick analysis of urine chemistry: benefits and limitations of dry chemistry-based assays. *Postgrad Med* 132(3):225–233. <https://doi.org/10.1080/00325481.2019.1679540>
- Klupfel J, Koros RC, Dehne K, Ungerer M, Wurstle S, Mautner J, Feuerherd M, Protzer U, Hayden O, Elsner M, Seidel M (2021) Automated, flow-based chemiluminescence microarray immunoassay for the rapid multiplex detection of IgG antibodies to SARS-CoV-2 in human serum and plasma (CoV-Rapid CL-MIA). *Anal Bioanal Chem* 413(22):5619–5632. <https://doi.org/10.1007/s00216-021-03315-6>
- Kristiansen KA, Potthast A, Christensen BE (2010) Periodate oxidation of polysaccharides for modification of chemical and physical properties. *Carbohydr Res* 345(10):1264–1271. <https://doi.org/10.1016/j.carres.2010.02.011>
- Lee HK, Lee BH, Dutta NK, Seok SH, Baek MW, Lee HY, Kim DJ, Na YR, Noh KJ, Park SH, Kariwa H, Nakauchi M, Mai LQ, Heo SJ, Park JH (2008) Detection of antibodies against SARS-coronavirus using recombinant truncated nucleocapsid proteins by ELISA. *J Microbiol Biotechnol* 18(10):1717–1721
- Li J, Liu WJ (2020) Puzzle of highly pathogenic human coronaviruses (2019-nCoV). *Protein Cell* 11(4):235–238. <https://doi.org/10.1007/s13238-020-00693-y>
- Paradiso AV, De Summa S, Loconsole D, Procacci V, Sallustio A, Centrone F, Silvestris N, Cafagna V, De Palma G, Tufaro A, Garrisi VM, Chironna M (2020) Rapid serological assays and SARS-CoV-2 Real-time polymerase chain reaction assays for the detection of SARS-CoV-2: comparative study. *J Med Internet Res* 22(10):e19152. <https://doi.org/10.2196/19152>
- Paul D, Gupta A, Rooge S, Gupta E (2021) Performance evaluation of automated chemiluminescence immunoassay based antigen detection: moving towards more reliable ways to predict SARS-CoV-2 infection. *J Virol Methods* 298:114299. <https://doi.org/10.1016/j.jviromet.2021.114299>
- Pawliczak R (2020) The immune response to SARS-CoV-2. Focus on severe COVID-19 pathogenesis. *Alergol Polska-Polish J Allergol* 7(3):146–152. <https://doi.org/10.1016/j.pulmoe.2021.03.008>
- Peto T, Uk C-LFO (2021) COVID-19: rapid antigen detection for SARS-CoV-2 by lateral flow assay: a national systematic evaluation of sensitivity and specificity for mass-testing. *Eclinicalmedicine* 36:100924. <https://doi.org/10.1016/j.eclinm.2021.100924>
- Rathe JA, Hemann EA, Eggenberger J, Li ZQ, Knoll ML, Stokes C, Hsiang TY, Netland J, Takehara KK, Pepper M, Gale M (2021) SARS-CoV-2 serologic assays in control and unknown populations demonstrate the necessity of virus neutralization testing. *J Infect Dis* 223(7):1120–1131. <https://doi.org/10.1093/infdis/jiaa797>
- Roychoudhury S, Das A, Sengupta P, Dutta S, Kolesarova A, Hleba L, Massanyi P, Slama P (2021) Viral pandemics of twenty-first century. *J Microbiol Biotechnol Food Sci* 10(4):711–716. <https://doi.org/10.3390/ijerph17249411>
- Sibai M, Solis D, Roltgen K, Stevens BA, Mfuh KO, Sahoo MK, Shi RZ, Zehnder J, Boyd SD, Pinsky BA (2021) Evaluation of SARS-CoV-2 total antibody detection via a lateral flow nanoparticle fluorescence immunoassay. *J Clin Virol* 139:104818. <https://doi.org/10.1016/j.jcv.2021.104818>
- Szunerits S, Pagneux Q, Swaidan A, Mishyn V, Roussel A, Cambillau C, Devos D, Engelmann I, Alidjinou EK, Happy H, Boukherroub R (2022) The role of the surface ligand on the performance of electrochemical SARS-CoV-2 antigen biosensors. *Anal Bioanal Chem*. <https://doi.org/10.1007/s00216-020-03137-y>
- Wang JFJ, Zhang N, Richardson SA, Wu JV (2021) Rapid lateral flow tests for the detection of SARS-CoV-2 neutralizing antibodies. *Expert Rev Mol Diagn* 21(4):363–370. <https://doi.org/10.1080/14737159.2021.1913123>
- Yin YY, Ma JJ, Tian XZ, Jiang X, Wang HB, Gao WD (2018) Cellulose nanocrystals functionalized with amino-silane and epoxy-poly(ethylene glycol) for reinforcement and flexibilization of poly(lactic acid): material preparation and compatibility mechanism. *Cellulose* 25(11):6447–6463. <https://doi.org/10.1007/s10570-018-2033-7>

**Publisher's Note** Springer Nature remains neutral with regard to jurisdictional claims in published maps and institutional affiliations.

Springer Nature or its licensor holds exclusive rights to this article under a publishing agreement with the author(s) or other rightsholder(s); author self-archiving of the accepted manuscript version of this article is solely governed by the terms of such publishing agreement and applicable law.